Preprints of the 19th World Congress
The International Federation of Automatic Control
Cape Town, South Africa. August 24-29, 2014

Real-time detection of Glucose Sensor and Insulin Pump Faults in an Artificial Pancreas.

Simone Del Favero *, **Marco Monaro** * **Andrea Facchinetti** *
Alessia Tagliavini * **Giovanni Sparacino** * **Claudio Cobelli** *

* *Department of Information Engineering, University of Padova, Via G. Gradenigo 6/B, 35131 Padova, Italy (phone: +39 049 827 7661; fax: +39 049 827 7699; e-mail: {sdelfave,marco.monaro,facchine,alessia.tagliavini,gianni,cobelli}@dei.unipd.it)*

Abstract: Sensors for real-time continuous glucose monitoring (CGM) and pumps for continuous subcutaneous insulin infusion (CSII) have opened new scenarios for Type 1 diabetes treatment, including the development of an Artificial Pancreas, a minimally invasive device for automated glycemic control via insulin infusion modulation. However, permanent or temporary faults of these two components, such as compression artifacts and pump-catheter occlusions, may expose diabetic patients to severe risks and strongly affect the efficacy of an automated treatment. In Facchinetti et al. [2013], a fault detection method was proposed, simultaneously exploiting CGM and CSII data streams and individualized models of glucose-insulin interaction. The method was assessed during night-time, a simple yet practically relevant case study where meals do not perturb glucose-insulin dynamics. In this contribution we extend the method from nighttime to whole day, facing the challenge of the meals and taking advantage of meal information commonly provided by the patient to the system. To this aim, the patient-specific model identified includes now meal as a further input of the system. The efficacy of the method is tested using the UVA/Padova Type 1 diabetic patient simulator.

1. INTRODUCTION

Type 1 Diabetes (T1D) is an autoimmune disease characterized by the destruction of pancreatic beta-cells that are responsible for insulin production, a crucial hormone for glucose metabolism. As a result, insulin needs to be administered exogenously to maintain glucose concentration in an optimal range so as to delay/minimize diabetes complications. In the last 30 years, we assisted to an important technological development of minimally invasive technologies for diabetes: pumps for continuous subcutaneous insulin infusion (CSII, [Pickup, 2012]) and sensors for real-time continuous glucose monitoring (CGM, [Bode and Battelino, 2010]), that opened new scenarios for Type 1 diabetes treatment, most notably enabling the development of the so-called Artificial Pancreas (AP), a closed-loop system for automated modulation of insulin infusion on the basis of CGM readings (Cobelli et al. [2011]).

However, permanent or temporary faults of either CGM or CSII, such as compression artifacts and pump-catheter occlusions, may expose diabetic patients to severe risks and strongly affect the efficacy of the automated treatment. This calls for the development of automated real-time fault detection tools producing effective and prompt alerts, allowing the timely adoption of suitable countermeasures and, thereby, mitigating the clinical impact of the faults.

Some notable attempts in this direction include the works of Bequette [2010], that proposed a fault detection method relying on CGM and capillary glucose measurements (obtained via finger pricks), and of Herrero et al. [2012], that employed CGM and carbohydrates ingestion data. Recently, Facchinetti et al. [2013], proposed a fault detection method simultaneously exploiting CGM and CSII data streams and individualized black-box models of glucose-insulin interaction. Faults were detected by checking for excessive discrepancy between predicted glycemic values and those measured by CGM. In Facchinetti et al. [2013] the method was assessed only during nighttime, a simple yet practically relevant case study where meals do not perturb glucose-insulin dynamics.

This contribution aims to extend the fault detection method of Facchinetti et al. [2013] to the whole day. To this aim, the method is modified to handle meals by taking advantage of meal information provided by the patient to the system, as requested by standard (manual) therapy and in many automated control implementations. In particular, suitable alarm strategies for different types of faults are proposed. The efficacy of the new fault-detection method is tested on simulated data, obtained using the UVA/Padova Type 1 diabetic patient simulator, [Kovatchev et al., 2008, Dalla Man et al., in press]. The faultless traces produced by the simulator where then corrupted with faults and the algorithm capability of detecting them without producing false alarms is assessed via specificity/sensitivity analysis.

⋆ This work was supported by ICT FP7-247138 Bringing the Artificial Pancreas at Home (AP@home) project.

2. FAULTS AFFECTING THE GLUCOSE SENSOR-INSULIN PUMP SYSTEM

In this section we will describe permanent and temporary faults commonly affecting CGMs and insulin pumps. Their impact on manual and automated therapy will be discussed to highlight the high clinical relevance of a prompt detection of these phenomena. In the work, we will only consider the faults that are not already automatically detected by the devices themselves. We will not consider on other highly-impacting types of CGM errors, such as inaccurate calibrations (inducing biases or stretching of the recorded dynamics) and slow accuracy drifts, as their compensation requires completely different approaches. On the contrary, we will consider gross errors affecting meal information provided by the patients to the system, in all respects a (rather critical) fault from a system perspective.

2.1 CGM sensor faults

In a CGM sensor, glucose measurement is performed via a glucose-oxidase reaction on a needle usually inserted in the abdominal tissue. Failures of the CGM sensor are mainly related to biomechanic issues of the sensor-tissue interface Helton et al. [2011]. In particular, motion of the patient and pressure on the sensor site can produce transient effects that can alter the glucose measurement. Spikes, i.e. isolated readings with abnormally large error, are usually due to motion of the patient and can be critical because can easily generate false crossing of the hypoglycemic threshold (70 mg/dl), unnecessarily triggering alarms.

Pressure application on the sensor (e.g., by rolling on the sensor while sleeping), alters the glucose-diffusion process in the insertion region and hence the sensitivity of the sensor, resulting in a systematic underestimation of glucose concentration for several minutes. These compression artifacts, called pressure-induced loss of sensitivity, are critical because they could trigger false hypoglycemic alerts and induce the AP controller to improperly suspend insulin infusion.

2.2 Insulin pump faults

Failures of the insulin infusion device can be due to mechanical defects [Guilhem et al., 2009] or to kinking, occlusion, and simple pulling out of the pump catheter from the insertion site [Schmid et al., 2010, van Bon et al., 2012]. Furthermore, in AP systems where the insulin pump is controlled wireless by a device running the control algorithm, persistent or recurrent communication faults may cause interruption or reduction of insulin delivery. Of note, the effect of an insulin pump fault becomes observable on glucose concentration profile only after tens of minutes (usually more than 40-50) since delays in insulin absorption and insulin action are present [Cobelli et al., 2009, Hovorka, 2006, Cobelli et al., 2011]. Apparently, such faults can be critical both for the safety of the patient and for the correct functioning of AP systems, since the reduced or missed delivery of insulin could lead to hyperglycemia and increases the risk of ketoacidosis [Guilhem et al., 2009]. Moreover, prolonged hyperglycemia following low/missed insulin can easily cause overcorrection and hypoglycemia, due to the emptying of insulin storage in the body and the consequent exacerbation of insulin action delay.

Although the majority of infusion related faults causes a reduction of infused insulin, there are also a few, yet very important, cases in which insulin injected is larger than the one the system is aware of, for instance if the infusion acknowledgment sent by the pump fails to reach the controller due to communication errors or if a misbehaving patient manually injects externally additional insulin.

2.3 Meal and meal-bolus faults

Controlling meal effects on blood glucose is a challenging disturbance rejection problem that patients have to face daily. At the time being, patients using CSII pumps deliver themselves a large insulin dose before each meal, usually called insulin bolus. The amplitude of this insulin pulse is proportional to the amount of carbohydrates estimated to be present in the upcoming meal, [Rosenbloom et al., 2008]. The carbohydrates-to-insulin ratio (CR) is patient-specific and provided to them by their diabetologist. Meal control is a major challenge also in automated insulin-infusion schemes, once again due to the large delay related to subcutaneous insulin injection route. As a consequence, a number of AP systems ask the patient to estimate carbohydrates content of the upcoming meal and to provide manually such an estimate to the controller (this procedure is usually called *meal announcement* [Cobelli et al., 2011]). In response to the announcement, the AP system delivers a pre-meal bolus. Patient compliance to meal bolus/announcement is critical to prevent post-prandial hyperglycemia [Burdick et al., 2004, Olinder et al., 2009], nonetheless it is difficult to enforce, especially for snacks and in adolescents [Olinder et al., 2011].

Meal faults, i.e. lack of consistency between estimated and actual meals, can be due to announcement omission or erroneous/multiple announcements, non-finished meal, vomiting or gross carbohydrates-estimation errors, strongly impacting on the effectiveness of the therapy.

Meal-triggered insulin boluses (from now on simply meal boluses), are affected by the above presented meal faults but might also be subject to the previously mentioned pump faults. Most frequently the consequence is an overestimation of the injected insulin, exposing the patient to risk of hyperglycemia, but sometimes faults might seldom result in an underestimation of the injected insulin with the consequent risk of hypoglicemia.

3. THE FAULT DETECTION METHOD

The block scheme of Fig.1 illustrates the architecture of the fault detection method, which conceptually consists of two separated modules. The first module is executed off-line and provides a Kalman-filter predictor identifying a patient-specific, linear, black-box model which describes the relationship between glucose concentration measured by CGM and the two considered inputs: insulin injected by the pump and carbohydrates assumed by the patient (meal). The second module works on-line and is in charge to generate faults alerts. To do so, the Kalman predictor, fed by measured CGM, CSII and meal data, provides

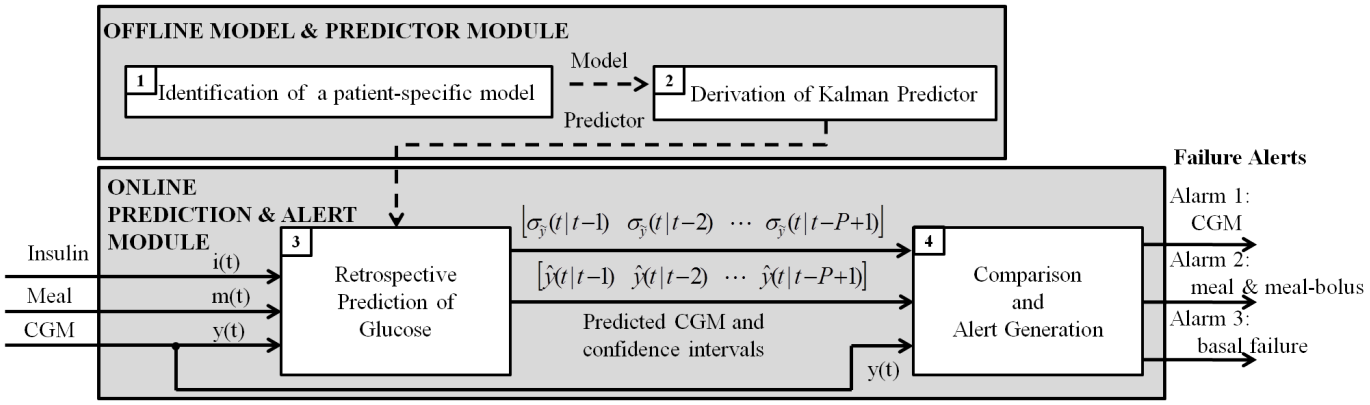

Fig. 1. A block scheme describing the architecture of the fault detection method. The *Offline Model&Predictor* module (top) performs the identification of glucose-insulin model and computes the the Kalman predictor. The *Online Prediction & Alert* module (bottom) performs the retrospective predictions of glucose concentrations (*Block 3*) and the comparison between predictions and measured CGM values to establish the presence of faults (*Block 4*).

at any time t the retrospective predictions of glucose concentration $\hat{y}(t|t-1), \hat{y}(t|t-2), \ldots, \hat{y}(t|t-P)$ together with their confidence interval. The alert generation module checks the consistency of these predictions with the corresponding actual measurements given by the CGM sensor and possibly generates a *fault alert*. A detailed description of fault detection method is reported in the following subsections 3.1 and 3.2.

3.1 Offline Model & Predictor Module

Both the identification of the glucose-insulin model (*Block 1* of Fig.1) and the derivation of the Kalman predictor (*Block 2* of Fig.1) are performed off-line from previously collected CGM, CSII and meal data of the patient. *Block 1* produces a discrete state-space model in the innovation form:

$$x(t+1) = Ax(t) + Bu(t) + Ke(t) \quad (1)$$
$$y(t) = Cx(t) + Du(t) + e(t) \quad (2)$$

where $x(t)$ is the $n \times 1$ state vector at discrete time t, the $u(t)$ is the 2×1 vector of inputs, $u(t) = [i(t),\ m(t)]^T$, where the scalar $i(t)$ is the insulin infusion rate (U/h) at time t (measured in U/h) and the scalar $m(t)$ is the carbohydrate ingestion, meal from now on, an impulsive signal equal to zero everywhere except at meal time, where it is equal to the estimated meal size. $e(t)$ is the scalar innovation process (white noise of variance σ_e^2 estimated from the data), $y(t)$ is the glucose level measured by the CGM sensor at time t (measured in mg/dl), A is the $n \times n$ state matrix, B is the $n \times 2$ input vector, K is the $n \times 1$ state-disturbance vector, C is the $1 \times n$ output matrix (in this case is a vector), and D is the 2×1 feed-forward matrix. The identification of unknown matrices A, B, C, D, and K of the model is performed resorting to a numerical algorithm for subspace state identification suitable for closed-loop systems such as the glucose-insulin one, see Katayama et al. [2005] and therein for further details.

The Kalman predictor can be obtained by simply computing, at each time instant t, the estimation of the future state vector $\hat{x}(t+1|t)$:

$$\hat{x}(t+1|t) = A\hat{x}(t|t-1) + Bu(t) + K(y(t) - \hat{y}(t|t-1)) \quad (3)$$

and using this value to estimate the 1-step ahead glucose prediction $\hat{y}(t|t-1)$:

$$\hat{y}(t|t-1) = C\hat{x}(t|t-1) + Du(t) \quad (4)$$

More details on the implementation can be found in Franklin et al. [1990].

3.2 Online Prediction & Alert Module

The Kalman predictor is applied in real time using the streams of CGM, CSII and meal data. In particular, for each t, the predictor is fed with the amounts of insulin injected till time t, meal consumed up to t, and with CGM data till time $t - P$, where P is the prediction horizion in steps (i.e, prediction PH minutes ahead, PH $= P \cdot T_s$, $T_s = 5$ [min] sampling time of the system). *Block 3* output is the "retrospective" prediction of all glucose concentrations from $t - P + 1$ to t, computed as:

$$\begin{aligned}\hat{y}(t-P+k|t-P) = {} & CA^{k-1}\hat{x}(t-P+1|t-P) + \\ & + C\sum_{i=1}^{k-1} A^{i-1}Bu(t-P+i) + Du(t-P+k)\end{aligned} \quad (5)$$

with $k = 1, ..., P$. *Block 3* allows also producing an estimate of the confidence interval for each of the predicted values $\hat{y}(t-P+k|t-P)$:

$$(\hat{y}(t-P+k|t-P) - m\sigma_{\tilde{y}_k}, \hat{y}(t-P+k|t-P) + m\sigma_{\tilde{y}_k}) \quad (6)$$

where $m = 3$ and $\sigma_{\tilde{y}_k} = \sqrt{C\Sigma_{\tilde{x}_k}C^T + \sigma_e^2}$ is the standard deviation of the $k-step$ ahead prediction value with $\Sigma_{\tilde{x}_k}$ the covariance matrix of the estimated state vector $\hat{x}(t-P+k|t-P)$. This means that, with the chosen parameters, assuming exact model and Gaussian innovation, the estimated confidence interval should contain about 99.5% of the CGM values, thus outliers and unexpected values will likely overcome it.

At each time instant t, *Block 4* compares the $k = 1, ..., P$ CGM values $y(t - P + k)$ with their retrospective predictions $\hat{y}(t - P + k|t - P)$ and confidence intervals. Three alarm strategies are used:

- *Alarm 1* of *Block 4* is an alarm for CGM fault (spikes or pressure-induced loss of sensitivity), obtained with $P = 1$. If the measurement falls outside the confidence interval of the 1-step ahead retrospective prediction, the sample is declared faulty. Furthermore, the measurement is not used in the measurement update step.
- *Alarm 2* checks if the above condition holds for 3 consecutive steps and, in this case, a second alarm is prompted. This alarm allows to detect reliably meal and meal bolus faults.
- *Alarm 3* returns a fault alert when $\forall k = 3, ..., 12$ CGM values $y(t - P + k)$ falls outside the corresponding retrospective prediction $\hat{y}(t - P + k|t - P)$ and confidence intervals. This alarm is used for basal infusion fault detection.

4. DATABASE

The following analysis is based on computer simulation (*in-silico* data), obtained by using the UVA/Padova Type 1 diabetic patient simulator, Kovatchev et al. [2008], Dalla Man et al. [in press]. This simulator was approved by the US Food and Drug Administration as a substitute of animal testing prior to closed-loop clinical trials on humans. The simulator was used to generate fault-free data from a population of $N = 100$ virtual subjects. For each subject, 6 days of closed-loop control with three meals per day, were simulated starting from 00:00. Breakfast, lunch and dinner took place at 07:30, 13:00, and 19:30, respectively with carbohydrates consumption of 50g, 60g and 80g respectively. A zero-mean colored Gaussian noise was added to the glucose profile to simulate measurement noise of CGM data, as proposed in Toffanin et al. [2013]. Continuous data were sampled with sampling time $T_s = 5$ min, a typical sampling time of CGM sensors and AP implementations.

The first 3 days of data were used for model training. The night of day 4 was used to perform Kalman filter initialization and was excluded from the analysis. The remaining 2.5 days (9 meals and 2 nights) were used to test the proposed algorithm, adding one fault episode for each patient at a random time instant. For each type of faults, several faults amplitudes and faults durations were considered, as described below

Scenario A (spikes)
An anomalously large error of amplitude A was added to the CGM reading at the random time t_f: $\mathrm{CGM}_{\mathrm{fualty}}(t_f) = \mathrm{CGM}(t_f) + A$, to simulate a CGM spike. The considered amplitudes were A=[−7.5,−10,−15,−20,−25] [mg/dl].

Scenario B (pressure-induced loss of sensitivity)
A sequence of consecutive large errors of amplitude A were added to the CGM readings from the random time t_f for a fixed duration D:

$$\mathrm{CGM}_{\mathrm{faulty}}(t_f, t_f + D) = \mathrm{CGM}(t_f, t_f + D) + A,$$

to simulate a pressure-induced loss of sensitivity. The considered amplitudes were A=[−7.5,−10,−15,−20,−25] [mg/dl] and the durations are $D = [10, 20, 30, 60]$ [min].

Scenario C (meal faults)
An error of relative amplitude E was added to one meal randomly selected among the 9 available:

$$m_{\mathrm{faulty}}(t_f) = m(t_f)(1 + E/100\%)$$

to simulate a meal estimation error. The considered relative amplitude are $E = [-100\%, -75\%, -50\%, -25\%, 0\%, 25\%, 50\%, 75\%, 100\%]$, spanning from a miss announcement (E=−100%) to the case in which only half of the announced meal were actually consumed (E=100%).

Scenario D (meal-bolus faults)
An error of relative amplitude E was added to one meal bolus randomly selected among the 9 available:

$$i_{\mathrm{faulty}}(t_f) = i(t_f)(1 + E/100\%).$$

The considered relative amplitude were $E = [-100\%, -75\%, -50\%, -25\%, 0\%, 25\%, 50\%, 75\%, 100\%]$, spanning from a bolus deliver but not recorded (i.e. missed meal bolus ackledgment, $E = -100\%$) to the case in which only half of the recorded insulin was actually injected (ex. partial occlusion, $E = 100\%$).

Scenario E (basal faults)
An error of relative amplitude E was added to modify the basal delivery from the random time t_f for a fixed duration D:

$$i_{\mathrm{faulty}}(t_f, t_f + D) = i(t_f, t_f + D)(1 + E/100\%).$$

Various relative amplitudes were considered, spanning from basal delivered but not recorded (missed injection acknowledgment, E=−100%) to the case in which only half of the recorded insulin was actually injected (ex. partial occlusion, $E = 100\%$).

Furthermore, in all scenarios we analyzed also the baseline case in which no fault was present, i.e. $A = 0$ or $E = 0$.

5. CRITERIA FOR METHOD ASSESSMENT

The performance of the fault detection method was assessed by a sensitivity and specificity analysis. For sake of clarity, let us focus first on Scenario A (spikes). For each time instant in which a CGM value is available, the fault-detection *alarm 1* could be either *on* or *off*. In case of alarm *on*, it was classified as true/false positive (TP/FP) depending on whether it did/did not happen in correspondence of a spike; in case of alarm *off*, it was classified as false/true negative (FN/TN) according to weather it did/did not occur in correspondence of a not-faulty sample. Moreover, we computed sensitivity,

$$\text{Sensitivity} = \frac{\text{TP}}{\text{TP+FN}},$$

representing the fraction of faults correctly detected and specificity,

$$\text{Specificity} = \frac{\text{TN}}{\text{TN+FP}},$$

accounting for the fraction of non-faulty samples correctly classified. Finally we computed accuracy, defined as

$$\text{Accuracy} = \frac{\text{TN+TP}}{\text{TN+FP+FN+TP}}.$$

Let us consider, then, bolus faults. For this type of fault, the sample-wise comparison of the alarm-signal with the fault/not-fault–signal proposed above is not meaningful. In fact, since the presence of delays in insulin absorption/action, the effect of the fault on glucose concentration will be observable only a few samples later and no alarm

		$A =$	0	-7.5	-10	-15	-20	-25
True Negative	TN		28111.00	28100.00	28091.00	28121.00	28100.00	28200.00
False Negative	FN		0.00	38.00	16.00	13.00	15.00	14.00
False Positive	FP		620.00	644.00	647.00	616.00	634.00	609.00
True Positive	TP		0.00	62.00	84.00	87.00	85.00	86.00
Sensitivity [%]	100·TP/(TP+FN)		NaN	62.00	84.00	87.00	85.00	86.00
Specificity [%]	100·TN/(FP+TN) [%]		97.79	97.76	97.75	97.86	97.79	97.89
Accuracy [%]	$100 \cdot \frac{TP+TN}{TP+FN+TN+FP}$		97.79	97.64	97.70	97.82	97.75	97.84

Table 1. Results of Scenario A: spikes.

	$D = 0$	$D = 10$ min					$D = 20$ min				
$A =$	0	-7.5	-10	-15	-20	-25	-7.5	-10	-15	-20	-25
TN	56783	18560	18559	18541	18559	18555	10925	10947	10923	10989	10967
FN	0.00	36.00	14.00	10.00	11.00	9.00	34.00	13.00	3.00	7.00	7.00
FP	917.00	543.00	535.00	528.00	535.00	533.00	456.00	449.00	446.00	430.00	426.00
TP	0.00	63.00	85.00	90.00	89.00	91.00	66.00	87.00	97.00	93.00	93.00
Sensitivity [%]	NaN	63.64	85.86	90.00	89.00	91.00	66.00	87.00	97.00	93.00	93.00
Specificity [%]	98.41	97.16	97.20	97.23	97.20	97.21	95.99	96.06	96.08	96.23	96.26
Accuracy [%]	98.41	96.98	97.14	97.19	97.16	97.18	95.73	95.98	96.09	96.21	96.23

	$D = 30$ min					$D = 60$ min				
$A =$	-7.5	-10	-15	-20	-25	-7.5	-10	-15	-20	-25
TN	7676	7693	7724	7748	7739	3968	3946	3923	3914	3902
FN	29.00	19.00	7.00	4.00	7.00	32.00	17.00	8.00	15.00	6.00
FP	409.00	406.00	399.00	375.00	391.00	354.00	370.00	410.00	418.00	414.00
TP	71.00	81.00	93.00	96.00	93.00	68.00	83.00	92.00	85.00	94.00
Sensitivity [%]	71.00	81.00	93.00	96.00	93.00	68.00	83.00	92.00	85.00	94.00
Specificity [%]	94.94	94.99	95.09	95.38	95.19	91.81	91.43	90.54	90.35	90.41
Accuracy [%]	94.65	94.82	95.06	95.39	95.16	91.27	91.24	90.57	90.23	90.49

Table 2. Results of Scenario B: pressure-induced loss of sensitivity.

can be prompted at fault time. As a consequence, a false negative will be unavoidable. Moreover, if a few samples later the fault is detected, this will count as a false positive in sample-wise analysis. To circumvent this difficulty, we consider time intervals of duration $4h$, synchronized with meal bolus. If fault-detection *alarm 2* detects a fault in this time block, then it counts as TP, otherwise as FN. If the meal/bolus-fault alarms is generated in any other 4h-time block, it will count as a FP. The same 4h-block analysis is used for meal faults. For the pressure-induced loss of sensitivity losses, a block analysis is performed on fault-detection *alarm 1*, with block duration equal to the duration of the loss under study.

6. RESULTS

Results of Scenario A are reported in Table 1. FP are limited (specificity above 97.5%) for all simulated amplitudes. Sensitivity is around 85%, except for amplitude $A = 7.5$ mg/dl, that makes the spike easily confoundable with CGM noise. Spike detection can be considered satisfactory, exhibiting only a slight deterioration with respect to night-only results found in Facchinetti et al. [2013]. Similar considerations emerge from Table 2, that reports results of Scenario B assessing pressure-induced sensitivity losses). Results of Scenario C are reported in Table 3 which demonstrates that the method is effective in detecting meal faults, reaching sensitivity around 90% when $|E| \geq 50\%$. Also insulin bolus faults (Scenario D, Table 4) are detected effectively, with sensitivity above 90% when $|E| \geq 75\%$. Specificity for meal/meal-boluses fault alarm is acceptable. Scenario E is certainly the most challenging set-up, due to the difficulties to identify models reliably predicting many steps ahead glycemic variation, as needed to account for the effect of basal failures on CGM traces. In view of this, *alarm 3* exhibited a limited number of FP (specificity around 90% in all tests), but its sensitivity reaches 50% only for long-duration faults ($D \geq 4$ hours) with large amplitues ($E = \pm 100\%$).

7. CONCLUSION

In this contribution we extend the fault detection method of Facchinetti et al. [2013] for whole day use, exploiting meal information. In particular, three suitable alarm strategies for different types of faults are proposed. In-silico assessment shows that the method is effective in detecting CGM and meal faults. Moreover it exhibits good sensitivity also to meal-bolus faults.

Future investigations will focus on identifying more reliable models, allowing to accurately predict 1-3h ahead, which is required to detect with improved sensibility basal faults. Moreover, the proposed method will have to be validated on the challenging set-up of real data.

ACKNOWLEDGEMENTS

We would like thank prof. L. Magni and his team, especially Dr. C. Toffanin and Mr. M. Messori, University of Pavia, IT, for helping us with closed-loop data generation.

REFERENCES

B.W. Bequette. Continuous glucose monitoring: real-time algorithms for calibration, filtering, and alarms. *J Diabetes Sci Technol*, 4(2):404–18, Mar 2010.

	$E =$	-100 %	-75 %	-50 %	-25 %	0 %	25 %	50 %	75 %	100 %
True Negative	TN	906.00	906.00	910.00	903.00	977.00	917.00	925.00	912.00	932.00
False Negative	FN	0.00	0.00	1.00	15.00	0.00	47.00	11.00	5.00	2.00
False Positive	FP	194.00	194.00	190.00	197.00	223.00	183.00	175.00	188.00	168.00
True Positive	TP	100.00	100.00	99.00	85.00	0.00	53.00	89.00	95.00	98.00
Sensitivity [%]	100·TP/(TP+FN)	100.00	100.00	99.00	85.00	NaN	53.00	89.00	95.00	98.00
Specificity [%]	100·TN/(FP+TN)	82.36	82.36	82.73	82.09	81.42	83.36	84.09	82.91	84.73
Accuracy [%]	$100 \cdot \frac{TP+TN}{TP+FN+TN+FP}$	83.83	83.83	84.08	82.33	81.42	80.83	84.50	83.92	85.83

Table 3. Results of Scenario C: meal fault.

	$E =$	-100 %	-75 %	-50 %	-25 %	0 %	25 %	50 %	75 %	100 %
True Negative	TN	917.00	919.00	908.00	922.00	977.00	904.00	904.00	928.00	931.00
False Negative	FN	5.00	7.00	22.00	47.00	0.00	20.00	7.00	3.00	3.00
False Positive	FP	183.00	181.00	192.00	178.00	223.00	196.00	196.00	172.00	169.00
True Positive	TP	95.00	93.00	78.00	53.00	0.00	80.00	93.00	97.00	97.00
Sensitivity [%]	100·TP/(TP+FN)	95.00	93.00	78.00	53.00	NaN	80.00	93.00	97.00	97.00
Specificity [%]	100·TN/(FP+TN)	83.36	83.55	82.55	83.82	81.42	82.18	82.18	84.36	84.64
Accuracy [%]	$100 \cdot \frac{TP+TN}{TP+FN+TN+FP}$	84.33	84.33	82.17	81.25	81.42	82.00	83.08	85.42	85.67

Table 4. Results of Scenario D: meal-bolus fault.

B. W. Bode and T. Battelino. Continuous glucose monitoring. *Int J Clin Pract Suppl*, (166):11–15, Feb 2010.

J. Burdick, H. P. Chase, R. H. Slover, K. Knievel, L. Scrimgeour, A. K. Maniatis, and G. J. Klingensmith. Missed insulin meal boluses and elevated hemoglobin A1c levels in children receiving insulin pump therapy. *Pediatrics*, 113(3 Pt 1):e221–224, Mar 2004.

C. Cobelli, C. D. Man, G. Sparacino, L. Magni, G. De Nicolao, and B. P. Kovatchev. Diabetes: Models, Signals, and Control. *IEEE Rev Biomed Eng*, 2:54–96, Jan 2009.

C. Cobelli, E. Renard, and B. Kovatchev. Artificial pancreas: past, present, future. *Diabetes*, 60(11):2672–2682, Nov 2011.

C. Dalla Man, F. Micheletto, D. Lv, M. Breton, B. Kovatchev, and C. Cobelli. The UVa/Padova type 1 diabetes simulator: new features. *J Diabetes Sci Technol*, in press.

A. Facchinetti, S. Del Favero, G. Sparacino, and C. Cobelli. An online failure detection method of the glucose sensor-insulin pump system: Improved overnight safety of type-1 diabetic subjects. *IEEE Transactions on Biomedical Engineering*, 60(2):406–16, Feb. 2013.

G. F. Franklin, J. D. Powell, and M. L. Workman. *Digital Control of Dynamic Systems, Second Edition*. Addison-Wesley, Boston, 1990.

I. Guilhem, B. Balkau, F. Lecordier, J. M. Malecot, S. Elbadii, A. M. Leguerrier, J. Y. Poirier, C. Derrien, and F. Bonnet. Insulin pump failures are still frequent: a prospective study over 6 years from 2001 to 2007. *Diabetologia*, 52:2662–2664, Dec 2009.

K. L. Helton, B. D. Ratner, and N. A. Wisniewski. Biomechanics of the sensor-tissue interface-effects of motion, pressure, and design on sensor performance and foreign body response-part II: examples and application. *J Diabetes Sci Technol*, 5:647–656, May 2011.

P. Herrero, R. Calm, J. Veh, J. Armengol, P. Georgiou, N. Oliver, and C. Tomazou. Robust fault detection system for insulin pump therapy using continuous glucose monitoring. *J Diabetes Sci Technol*, 6(5):1131–41, Sep 2012.

R. Hovorka. Continuous glucose monitoring and closed-loop systems. *Diabet. Med.*, 23:1–12, Jan 2006.

T. Katayama, H. Kawauchi, and G. Picci. Subspace identification of closed-loop systems by orthogonal decomposition. *Automatica*, 41:863–872, May 2005.

B.P. Kovatchev, M.D. Breton, C. Cobelli, and C. Dalla Man. Method, system and computer simulation environment for testing of monitoring and control strategies in diabetes. Patent WO/2008/157781, 2008.

A. L. Olinder, A. Kernell, and B. Smide. Missed bolus doses: devastating for metabolic control in CSII-treated adolescents with type 1 diabetes. *Pediatr Diabetes*, 10 (2):142–148, Apr 2009.

A. L. Olinder, K. T. Nyhlin, and B. Smide. Reasons for missed meal-time insulin boluses from the perspective of adolescents using insulin pumps: 'lost focus'. *Pediatr Diabetes*, 12(4 Pt 2):402–409, Jun 2011.

J. C. Pickup. Insulin-pump therapy for type 1 diabetes mellitus. *N. Engl. J. Med.*, 366(17):1616–1624, Apr 2012.

A. L. Rosenbloom, J. H. Silverstein, S. Amemiya, P. Zeitler, and G. J. Klingensmith. Insulin treatment. ISPAD Clinical Practice Consensus Guidelines 2006-2007. Type 2 diabetes mellitus in the child and adolescent. *Pediatr Diabetes*, 9(5):512–526, Oct 2008.

V. Schmid, C. Hohberg, M. Borchert, T. Forst, and A. Pfutzner. Pilot study for assessment of optimal frequency for changing catheters in insulin pump therapy-trouble starts on day 3. *J Diabetes Sci Technol*, 4:976–982, Jul 2010.

C. Toffanin, M. Messori, F. Di Palma, G. De Nicolao, C. Cobelli, and L. Magni. Artificial pancreas: MPC design from clinical experience. *Journal of Diabetes Science and Technology*, 7(6):1470–1483, Nov 2013.

A. C. van Bon, D. Dragt, and J. H. Devries. Significant time until catheter occlusion alerts in currently marketed insulin pumps at two Basal rates. *Diabetes Technol. Ther.*, 14(5):447–448, May 2012.